2017 American Control Conference
Sheraton Seattle Hotel
May 24–26, 2017, Seattle, USA

On Identifying the Aging Mechanisms in Li-ion Batteries Using Two Points Measurements

Peyman Mohtat, Farinaz Nezampasandarbabi, Shankar Mohan, Jason B. Siegel, and Anna G. Stefanopoulou

Abstract— **Lithium-ion batteries are prone to aging, which decreases the battery performance. The term battery State of Health (SOH) is widely used to describe many different aspects of battery performance. One critical aging characteristic is the loss of cyclable energy quantified by the decrease in capacity. Algorithms that estimate the capacity fade using voltage measurements are widely published in literature and are commonly used in commercial Battery Management Systems (BMS). However, there are fewer studies identifying the aging mechanisms, such as the loss of cyclable lithium, or the loss of active material, both of which manifest as capacity fade. Furthermore, many of these algorithms require voltage measurement data acquired during a full charge or discharge cycle, which is inconvenient to obtain while the battery is in use. In the following, we present a methodology to identify the aging mechanisms by changes in the capacity of active material in each electrode, and the changes in the stoichiometric operating window of the half-cell potentials. The proposed method utilizes measurement obtained from only two operating points, with no requirement on a constant current while traversing between these two operating points. The method is tested via simulating the LiFePO4 (LFP) chemistry, where identification is particularly difficult due to its flat voltage characteristics. Furthermore, unlike previously presented methods, the identifiability of the aging mechanisms is studied with respect to location of the two operating points in the voltage curve. It is important to note that the techniques explored and proposed in this paper rely on opportunistic measurements of terminal voltage after a rest period due to its reliance on the invariant characteristic of the half-cell potentials.**

I. Introduction

The use of lithium ion batteries is growing every day, and nowadays they are found in most consumer electronics, and car manufacturers are moving from the fossil fuel powered cars to electric power cars at a rapid speed. However, despite the increase in battery research, there are still a number of hurdles that have yet to be resolved.

One major issue is the reduction in cell capacity over time. This capacity fade is one of the key indicators of the cell State of Health (SOH). Furthermore, accurately measuring and predicting SOH is very important in a Battery Management System (BMS) to have a sound estimate of the battery performance. Many studies have focused their attention to find and develop tools for battery SOH estimation; the authors of [1] present an excellent review of the many methods that have been proposed and delineates their advantages and disadvantages.

One of the important aspects of SOH estimation is not only to give a measure of the current capacity of the cell, but also to detect the aging mechanisms causing the capacity fade. Be it a laboratory tool or a diagnostic technique performed after occasional periods of rest, knowing more about the cause of capacity fade would help inform decisions about how to prevent further degradation. There can be many factors responsible for battery aging such as Loss of Cyclable Lithium (LCL), Loss of Active Material (LAM), and increase in resistance, to name a few [2]. Growth of the Solid Electrolyte Interphase (SEI) can cause LCL, which is mostly observed in the initial stages of aging [2]. This loss would mean, for instance, during discharge the cathode would be less lithiated and would be at more positive voltage. To reach the minimum terminal voltage the cell would have to operate at a higher anodic potential as shown in Figure 1 or lower anode stoichiometry (less lithium per carbon atoms). Therefore, by keeping the cell operating voltage limits constant, a shift would be introduced in the starting point of the potential curve of anode with respect to the cathode. Furthermore, there are studies that postulate that as the cell ages, the half-cell potential of the anode and cathode would move or slip with respect to each other [3], [4]. The physical phenomena responsible for LAM can also be categorized into different types and according to the affected electrode [2], for example particle fracture, and loss of contact with current collector.

Voltage based capacity estimation techniques have been used extensively, and can track relative changes in each electrode through shifting of the peaks in the Incremental Capacity (IC) curves [5], [6]. It is also known that the peaks observed in the dV/dQ are associated with the phase transitions in the anode and cathode. In [2], [7], the authors use measurements of the terminal voltage obtained during slow charging of the cell, over the entire operating range to identify the different aging mechanisms for several different cell chemistries.

In [3], [8] the authors have showed the aging can be identified with the Differential Voltage (DV) curves, and for NMC cells have calculated the different DV curves by shifting the half-cell potentials of the cell relative to each other. In [9] a method is proposed through fitting the charging cell voltage curves (CCVC) using transformation, which estimates the capacity of the cell. In [4] the authors used only two voltages measurement and developed a tool for the cell state of health (SOH) estimation. However, they have only considered one aging mechanism namely the Loss of

P. Mohtat, F. N., J.B. Siegel, & A.G. Stefanopoulou are with the Department of Mechanical Engineering, University of Michigan, Ann Arbor, MI 48109 {pmohtat,siegeljb,annastef}@umich.edu, farinaz.ne@gmail.com

S. Mohan is with the Department of Electrical Engineering and Computer Science, University of Michigan, Ann Arbor, MI 48109 elemsn@umich.edu

978-1-5090-5992-8/$31.00 ©2017 AACC

Cyclable Lithium.

The contributions of this paper can be summarized as follows: a methodology to identify the aging mechanism in Lithium-ion batteries using the stoichiometric operating window and capacity of the electrodes. An optimization problem to estimate the stoichiometric operating window and capacity of the electrodes. The proposed technique requires information at two operating points, and the net Ampere-hours expended in traversing between these points, which can be obtained by coulomb counting. The main advantage of the method proposed in this paper is that there is no need for a constant charge or discharge, any drive cycle will do as long as we are doing the coulomb counting. Furthermore, to our knowledge, we present a first study on the identifiability of the aging mechanisms using the information provided from selection of different voltage pairs.

This paper is organized as follows: Section II describes the aging mechanisms and the model to identify them considered in this work. Section III presents a technique to estimate the parameters of the model employed in this study. Section IV demonstrates the method effectiveness using an example of an LFP cell, and discusses the identifiability of the aging mechanism with respect to the provided information sets. Section V summarizes the contributions.

II. A MODEL FOR BATTERY AGING MECHANISM IDENTIFICATION

There are several mechanisms responsible for battery aging. In this paper, we focus our attention to the following two: Loss of Cyclable Lithium (LCL), and Loss of Active Material (LAM). In this section, we present a model to identify some of the key parameters that affect the terminal voltage and discuss the impact of the aging mechanism has on these parameters.

Let the stoichiometric *state* of the anode and cathode, be denoted by x and y, respectively. Furthermore, let $y, x \in [0, 1]$. As an example, for the anode the chemical formula is Li_xC_6, which means at fully intercalated state, ($x = 1$), there is one lithium atom per six carbon atoms. However, due to manufacturing requirements, different cell specification, initial SEI formation, and etc., x and y are not necessarily from 0 to 1. Hence, the term the stoichiometry window is introduced for each electrode. The window for anode is delineated with x_0 for the fully lithiated state (for cathode y_0 for the fully delithiated state) and x_{100} for the fully delithiated state (for cathode y_{100} for the fully lithiated state).

Let the half-cell potentials of the cathode and anode, measured against Lithium, as a function of x and y, be denoted by $U_p(y)$ and $U_n(x)$, respectively. Then, while the cell is in electrical equilibrium (no current is drawn and the voltage is in steady state), the terminal voltage of the cell is equal to Open Circuit Potential (OCV) and satisfies the following.

$$U_p(y) - U_n(x) = V_t \tag{1}$$

Then, the stoichiometric window of each electrode, $(x_0, y_0, x_{100}, y_{100})$, satisfies the relation

$$U_p(y_0) - U_n(x_0) = V_{min}, \tag{2}$$

$$U_p(y_{100}) - U_n(x_{100}) = V_{max}. \tag{3}$$

Where V_{min} and V_{max} is the minimum and maximum operating voltage of the cell, respectively. Furthermore, the stoichiometric *state* of each electrode, (x, y) satisfies the following relation

$$y = y_0 - Q/C_p, \quad x = x_0 + Q/C_n. \tag{4}$$

where C_p and C_n are the total capacities of positive electrode (cathode) and negative electrode (anode), respectively. Q is the coulomb counting from the fully discharged state (for convenience, all measured in Ampere-hours). The total

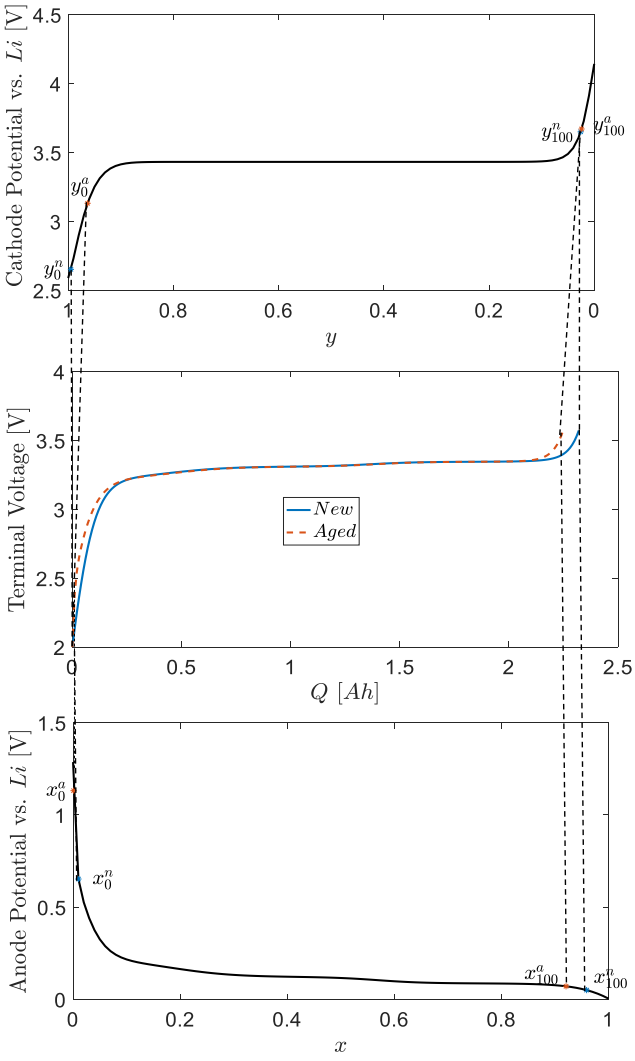

Fig. 1. The breakdown of cell terminal voltage into the contribution of individual electrodes and identification of the corresponding stoichiometric operating windows for a new (blue) and an aged (red) cell. The superscript *n*, and *a* correspond to the new and aged cell respectively. The figure is showing the aging caused by LCL (case 1 in Table I). Notice that in this case, the minimum stoichiometric *state* of the anode has decreased in the aged cell because of a LCL.

capacity of the cell, C, is measured as the total capacity that be added (removed) to (from) the cell as it operates between its voltage limits. It follows from Eq. (4) that, with $(x_0, y_0, x_{100}, y_{100})$ as stoichiometric windows of the electrodes, the following equality is true.

$$C = C_p \cdot (y_0 - y_{100}) = C_n \cdot (x_{100} - x_0) \tag{5}$$

According to Dubarry, et al. [2], LAM can be divided into four subcategories: (1) lithiated in positive electrode, (2) delithiated in positive electrode, (3) lithiated in negative electrode, (4) delithiated in negative electrode. Furthermore, LCL is also divided into two subcategories during; (1) charging in negative electrode, and (2) discharging in positive electrode. However, in this paper, similar to the approach in [7], we only consider LAM as the changes in active material. Meaning a change in $C_p(C_n)$ signifies LAM in cathode(anode). Furthermore, we only consider LCL happening at either charging or discharging. Meaning we only consider changes in (x_0, y_0) or (x_{100}, y_{100}) as LCL.

The preceding simplification, enables separation of the effects of LAM and LCL on the stoichiometric operating windows. Hence the ability to identify the aging mechanisms. The forthcoming discussion is based the assumption that LCL only influences (x_0, y_0), however, a similar approach can also be applied when LCL only influences (x_{100}, y_{100}). The following presentation explains impacts of each individual aging mechanism on the parameters when they occur by themselves.

Suppose the cell ages because of LAM in the cathode. As an immediate consequence, C_p decreases to C_p', and the capacity, C, decreases. However, since there is no LCL happening , x_0 and y_0 do not change. The capacity is computed by substituting for (x_{100}, y_{100}) from Eq. (5) in Eq. (3), with C_p' instead of C_p, and solving for C

$$U_p\left(y_0 + \frac{C}{C_p'}\right) - U_n\left(x_0 - \frac{C}{C_n}\right) = V_{max} \tag{6}$$

Similarly, if the LAM is also happening in the anode, C_n decreases to C_n', and C is computed by using C_n' in the equation above as well.

Now, consider the alternate scenario in which the electrodes undergoes LCL; Suppose the cell is discharging, which means the Lithium atoms are moving from the anode (delithiation) to the cathode (lithiation). Due to phenomena like SEI formation some of the lithium would be lost, and it would not get stored in the cathode. Which means when the anode reaches x_0, the cathode is at a smaller y_0 (larger voltage). Consequently, since the cell is discharged until it hits the minimum voltage limit, x_0 moves to the left/decrease in the half-cell potential (Refer to Fig. 1), and y_0 moves to the right/decrease.

Furthermore, a smaller x_0, with C_p and C_n unchanged while satisfying Eqns. (2), (3), and (5), results in a smaller capacity and a change in the stoichiometric window of the anode and cathode similar to Fig. 1. In summary, LCL causes the stoichiometric window of the cathode to shift to the right, and the stoichiometric window of the anode to shift to the left.

	LCL	LAM			
Case		A	C	Changed	Unchanged
1	✓	✗	✗	$x_0, x_{100}, y_0, y_{100}, C$	C_p, C_n
2	✗	✓	✗	x_{100}, y_{100}, C_n, C	x_0, y_0, C_p
3	✗	✗	✓	x_{100}, y_{100}, C_p, C	x_0, y_0, C_n
4	✓	✓	✗	$x_0, x_{100}, y_0, y_{100}, C_n, C$	C_p
5	✓	✗	✓	$x_0, x_{100}, y_0, y_{100}, C_p, C$	C_n
6	✓	✓	✓	$x_0, x_{100}, y_0, y_{100}, C_n, C_p, C$	

TABLE I

SCENARIO LIST OF DIFFERENT AGING MECHANISMS AND THE PARAMETERS THAT CHANGE AS A CONSEQUENCE.

Table I collates the list of the different permutations of aging mechanisms and relates them to the parameters that change. From Table I, note that, if estimates of the different parameters is available, it is possible to identify LAM — if the capacity of an electrode has decreased, then LAM has occurred in that electrode. On the other hand, if the values of x_0 and y_0 have changed then LCL has contributed to the decrease in the capacity of the cell. This then can be used as a model to identify the aging mechanism that has caused a loss in capacity.

III. PARAMETER ESTIMATION

In this section, a method that relies on measurements obtained from two operating points will be presented. Let the stoichiometric state in each electrode, corresponding to each of these voltages be (x_1, y_1) and (x_2, y_2), that is using Eq. (1) the voltages V_1 and V_2 satisfy:

$$\begin{aligned} U_p(y_1) - U_n(x_1) &= V_1, \\ U_p(y_2) - U_n(x_2) &= V_2 \end{aligned} \tag{7}$$

Given information on the net amount of Ampere-hours drawn from the cell in traversing between the two voltages, ΔQ, it is easy to see that the stoichiometric states satisfies the relation:

$$\begin{aligned} x_2 &= x_1 + \frac{\Delta Q}{C_n}, \\ y_2 &= y_1 - \frac{\Delta Q}{C_p} \end{aligned} \tag{8}$$

Furthermore, here and hereafter, it is assumed that the cell does not degrade discernibly whilst the cell is traversing between the two voltages. Now let the cell capacity *state* when at voltage V_1, and V_2 be represented by Q_1, and Q_2, respectively [refer to Fig. 2]. Then, the following constraints are satisfied:

$$\begin{aligned} x_1 &= x_0 - \frac{Q_1}{C_n}, \quad y_1 = y_0 + \frac{Q_1}{C_p}, \\ x_2 &= x_0 - \frac{Q_2}{C_n} = x_0 - \frac{Q_1 + \Delta Q}{C_n}, \\ y_2 &= y_0 + \frac{Q_2}{C_p} = y_0 + \frac{Q_1 + \Delta Q}{C_p}. \end{aligned} \tag{9}$$

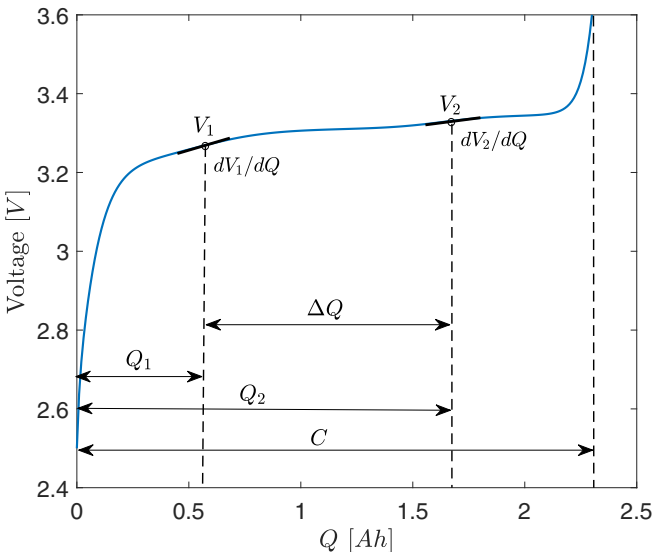

Fig. 2. A visual representation of the unknown quantities in the proposed algorithm.

Using these equations it is possible to substitute for (x_1, x_2, y_1, y_2) in Eqn. (7), and write down the equations as the following

$$U_p(y_0 + \frac{Q_1}{C_n}) - U_n(x_0 - \frac{Q_1}{C_p}) = V_1 \tag{10}$$

$$U_p(y_0 + \frac{Q_1 + \Delta Q}{C_p}) - U_n(x_0 - \frac{Q_1 + \Delta Q}{C_n}) = V_2 \tag{11}$$

The equation for the derivative of terminal voltage with respect to Ampere-hours, dV_1 and dV_2, at voltages V_1 and V_2, can also be related to the unknown parameters via the following equations:

$$-\frac{dU_p(y_0 + \frac{Q_1}{C_p})}{C_p} - \frac{dU_n(x_0 - \frac{Q_1}{C_n})}{C_n} = dV_1 \tag{12}$$

$$-\frac{dU_p(y_0 + \frac{Q_1+\Delta Q}{C_p})}{C_p} - \frac{dU_n(x_0 - \frac{Q_1+\Delta Q}{C_n})}{C_n} = dV_2 \tag{13}$$

where dU_p and dU_n are the rate change of the half-cell potential with respect to the stoichiometric *state* of the cathode, and anode, respectively. These equations provide the necessary additional information to identify the unknowns that define the operating window of the half-cells, and capacity, (x_0, y_0, C_n, C_p).

In addition to the unknown parameters, the capacity state at voltage V_1, Q_1 is also unknown. In other words, the position of the voltage measurements in the voltage curve is assumed to be unknown. These parameters can be estimated by solving the following optimization problem

$$\begin{aligned} &\min_{\theta} \sum_{i=1}^{4} \|\hat{Y}_i - Y_i\|^2 + \|\theta - \theta_0\|^2_W, \qquad (P) \\ &\text{st. } \theta \in \Theta, \\ &U_p(y_0) - U_n(x_0) = V_{min} \end{aligned}$$

where $\theta = [x_0, y_0, C_n, C_p, Q_1]$ is the vector of parameters to be estimated, The function $\hat{Y}_i$ is the function comprised of left-hand-sides of Eqns. (10)–(13), respectively. The place holder Y_i is the provided data indexed to match $\hat{Y}_i$.

The second term in (P) is a regularization term, such that $\forall x \in \mathbb{R}^n$, $W \in \mathbb{M}_+^{n\times n}$, $\|x\|^2_W := x'Wx$. In this work, W is picked as a constant number such that the first term and regularizing term in (P) are of same order.

The a priori estimate of the parameters is denoted by θ_0 in problem (P). This information is assumed available by virtue of the following facts: (1) used normally, the cell does not age significantly in a short period of time (within a few days); (2) the parameters for a new cell are identifiable with relative ease, and these parameters will usually be updated online; i.e. estimation is not performed in an information vacuum. The keen reader will recognize the similarity between (P) and the moving horizon estimator [10] [11].

The second constraint is the Eq. (2), which is the equation for the minimum voltage of the cell.

Finally, after finding the parameters, the following equation can be solved to estimate the capacity of the cell C, which is rewritten using the maximum voltage Eq. (3).

$$U_p(y_0 - \frac{C}{C_p}) - U_n(x_0 + \frac{C}{C_n}) = V_{max} \tag{14}$$

IV. Empirical estimability in an LFP cell

The problem introduced in Section III is used to identify the parameters of the voltage characteristic; and hence identify if an underlying aging mechanism has occurred. The solvability of problem (P) and the uniqueness of its solution depends on the *measurements*.

In this section, we consider a Lithium Iron Phosphate (LFP) cell as an example to demonstrate the proposed algorithm. The model of the cell is synthesized using the half-cell potential functions presented in [12] (reproduced in Eqns. (15)). The operating terminal voltage window is taken to be $[V_{min}, V_{max}] = [2.5, 3.6]$ V. The parameters used in the simulations are presented in Tab. II, and the open circuit potential of the this cell is shown in Fig. 2.

Observe from Fig. 2 that the open circuit voltage is almost flat in the middle region. For measurements obtained in this region some of the parameters are not identifiable. In this section, we aim to empirically identify which of the parameters can be identified with some epsilon accuracy, and when.

Specifically, we seek to identify, the pairs of terminal voltage measurements and corresponding OCV derivatives such that the parameter estimation error is 0.1% when the a priori guess is within 1% of the true solution. To achieve this, the range of cell capacity is discretized, and for each pair of distinct values of the cell's capacity, the corresponding open circuit potential and its derivatives are aggregated, and problem (P) is solved. The built-in MATLAB function *fmincon* (with the *sqp* solver) is utilized to solve (P), and the relative error of the parameter estimates are noted. Figure 3 presents the results of these trials.

$$
\begin{aligned}
U_n(x) =& 0.6379 + 0.5416exp(-305.5309x) - 0.044tanh(\frac{x-0.1958}{0.1088}) - 0.1978tanh(\frac{x-1.0571}{0.0854}) \\
&- 0.6875tanh(\frac{x+0.0117}{0.0529}) - 0.0175tanh(\frac{x-0.5692}{0.0875}) \\
U_p(y) =& 3.4323 - 0.8428exp(-80.2493(1-y)^{1.3198}) - 3.2474 \times 10^{-6}exp(20.2645(1-y)^{3.8003}) \\
&+ 3.2482 \times 10^{-6}exp(20.2646(1-y)^{3.7995})
\end{aligned} \tag{15}
$$

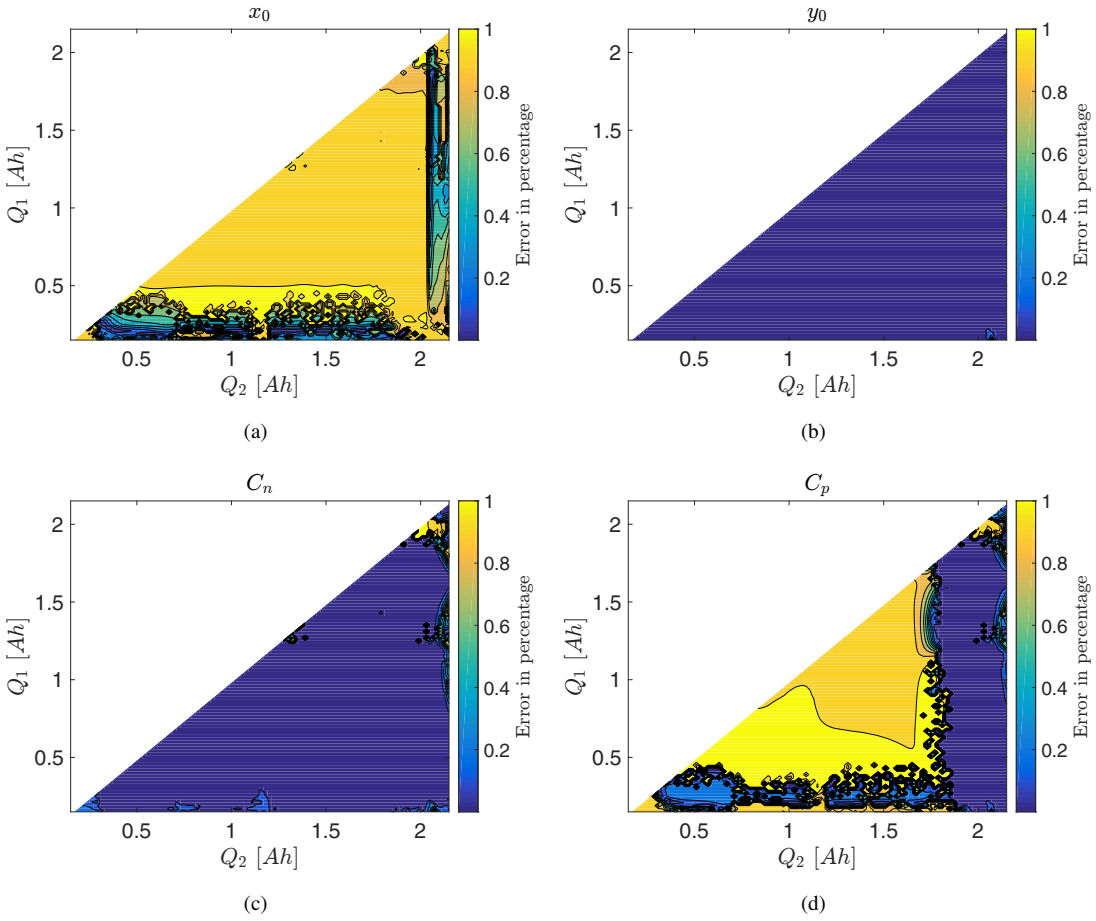

Fig. 3. Relative error for x_0 (a), y_0 (b), C_n (c), and C_p (d), by solving (P) for various voltage pair measurements depicted versus capacity state, the initial guess is with 1% deviation from the true value.

Parameter	LFP cell
x_0	0.0050
x_{100}	0.80
y_0	0.9421
y_{100}	0.0229
C_n (Ahrs)	2.8931
C_p (Ahrs)	2.5022
C (Ahrs)	2.30

TABLE II

PARAMETERS OF THE SYNTHESIZED CELL USED IN THE SIMULATION

Figures 3(a) and 3(b) paint different pictures of the estimability of x_0 and y_0. While the relative error in estimating the latter is small, almost everywhere, the same cannot be said for the former. In fact, the error in estimating y_0 is almost always smaller, and the difference between the two is more pronounced when measurements are obtained from the 'flat' regions of the OCV curve.

Recall that the objective function of problem (P) includes a weighted regularization term (with weights chosen such as to normalize the entries) that ensures that the optimal solution does not deviate far from the a priori estimate when a parameter cannot be estimated. In the 'flat' region of the OCV curve, the estimation error for x_0 is near 1% – close to the a priori estimate of x_0. This suggests that x_0 cannot be estimated when both operating points are in the flat region of the curve. However, for those voltage pairs that include one or both measurements from the shoulder or neck region of the voltage curve (the shoulder and neck are the regions at the start and end of the voltage curve with large gradients with respect to cell capacity, respectively) estimating x_0 is possible.

The reason for this disparity in estimating x_0 and y_0 can

be explained as follows. The parameters x_0 and y_0 are intrinsically coupled through the equality constraint in problem (P) (minimum voltage limit). Comparing the sensitivity of this constraint with respect to the unknowns, it is apparent that in the shoulder region of the OCV, $\frac{\partial U_p}{\partial y}$ is larger than $\frac{\partial U_n}{\partial x}$; i.e. this constraint is more sensitive to changes in y_0 than x_0. Furthermore, through simulations, it is noted that small changes to y_0 result in a discernible variation between the resultant OCV curves, even in the flat regions. Taken together, this suggests that y_0 can be estimated with small error. Finally, since the sensitivity of the terminal voltage with respect to x_0 is smaller (than that of y_0) in the shoulder region (V_{min} constraint), it stands to reason that x_0 has larger estimation error than y_0.

In Figs. 3(c), and 3(d) the resulting estimation errors for C_n and C_p are presented. Notice that the patterns in distribution of errors of C_p and C_n are similar to those of x_0 and y_0, respectively. The sensitivity with respect to C_p, and C_n can be written as $\frac{\partial U_p}{\partial y}\frac{Q_1}{C_p^2}$, and $\frac{\partial U_n}{\partial x}\frac{Q_1}{C_n^2}$. In the flat region $\frac{\partial U_p}{\partial y}$ is almost zero, compare to $\frac{\partial U_n}{\partial x}$. In the shoulder and neck region the magnitude of $\frac{\partial U_p}{\partial y}$ and $\frac{\partial U_n}{\partial x}$ are comparable. As a result, the voltage equation is less sensitive to variations in C_p in flat region compared to shoulder and neck region. Furthermore, the sensitivity is also multiplied by Q_1, so with a larger Q_1 the sensitivity would also be larger. Hence the reason behind C_p having a smaller estimation error in neck region compared to shoulder region.

As described in Section II, LCL and LAM aging mechanisms can be detected by identifying changes to some subset of the parameters (x_0, y_0, C_p, C_n). Since y_0 and C_n can be estimated within small error tolerance range, the conclusion follows: identifying LCL, and LAM in anode is possible. However, identifying LAM in cathode is only possible with measurement in shoulder and neck region.

V. Conclusion

In this paper, we present a methodology to identify the aging mechanisms associated with capacity loss in a lithium-ion battery. A model was proposed that relates changes in the capacity of active material and the stoichiometric operating window in each electrode to the aging mechanisms. The parameter estimation problem was then formulated as an optimization problem. The algorithm is different from traditional approaches in that it uses voltage measurements from only two operating points to estimate the parameters relating to the capacity of active material and the stoichiometric operating window. The algorithm was evaluated using simulations of a Lithium Iron Phosphate cell. The results indicate that one can identify LAM in anode and LCL. However, identifying LAM in cathode is only possible when measurements were obtained from regions with a large derivative in voltage with respect to capacity change.

Directions for further investigations: For a new cell with use of the full voltage curve, the parameters that identify the aging mechanisms could be estimated [7]. Using the parameters of the new cell, with a recursive scheme, we can keep track of the changes in parameters, while the cell is in use. Furthermore, we can use methods described in [13] to partition the parameters based on their estimability, for faster computation time.

To address the low observability in the flat voltage regions the addition of measurements from strain or force sensors could provide additional information. Similar to the half-cell potentials the total expansion of a cell, could also be taken as the sum of the half-cell expansion of the electrodes. However, we need to have a mechanical model of the cell in order to model the effects of the components of the cell like the separator, casing, and etc. on the force measurements. Approaches to model the mechanical behavior of the cells in the packs has been presented in [11], which can be used as a basis for a cell model.

References

[1] M. Berecibar, I. Gandiaga, I. Villarreal, N. Omar, J. V. Mierlo, and P. V. den Bossche, "Critical review of state of health estimation methods of li-ion batteries for real applications," *Renewable and Sustainable Energy Reviews*, vol. 56, pp. 572 – 587, 2016.

[2] M. Dubarry, C. Truchot, and B. Y. Liaw, "Synthesize battery degradation modes via a diagnostic and prognostic model," *Journal of Power Sources*, vol. 219, pp. 204 – 216, 2012.

[3] I. Bloom, L. K. Walker, J. K. Basco, D. P. Abraham, J. P. Christophersen, and C. D. Ho, "Differential voltage analyses of high-power lithium-ion cells. 4. cells containing {NMC}," *Journal of Power Sources*, vol. 195, no. 3, pp. 877 – 882, 2010.

[4] D. D. Domenico, P. Pognant-Gros, M. Petit, and Y. Creff, "State of health estimation for nca-c lithium-ion cells," *IFAC-PapersOnLine*, vol. 48, no. 15, pp. 376 – 382, 2015.

[5] A. J. Salkind, C. Fennie, P. Singh, T. Atwater, and D. E. Reisner, "Determination of state-of-charge and state-of-health of batteries by fuzzy logic methodology," *Journal of Power Sources*, vol. 80, pp. 293 – 300, 1999.

[6] C. Weng, Y. Cui, J. Sun, and H. Peng, "On-board state of health monitoring of lithium-ion batteries using incremental capacity analysis with support vector regression," *Journal of Power Sources*, vol. 235, pp. 36 – 44, 2013.

[7] X. Han, M. Ouyang, L. Lu, J. Li, Y. Zheng, and Z. Li, "A comparative study of commercial lithium ion battery cycle life in electrical vehicle: Aging mechanism identification," *Journal of Power Sources*, vol. 251, pp. 38 – 54, 2014.

[8] I. Bloom, A. N. Jansen, D. P. Abraham, J. Knuth, S. A. Jones, V. S. Battaglia, and G. L. Henriksen, "Differential voltage analyses of high-power, lithium-ion cells: 1. technique and application," *Journal of Power Sources*, vol. 139, no. 1, pp. 295 – 303, 2005.

[9] Y. Zheng, L. Lu, X. Han, J. Li, and M. Ouyang, "Lifepo4 battery pack capacity estimation for electric vehicles based on charging cell voltage curve transformation," *Journal of Power Sources*, vol. 226, pp. 33 – 41, 2013.

[10] C. V. Rao, J. B. Rawlings, and D. Q. Mayne, "Constrained state estimation for nonlinear discrete-time systems: stability and moving horizon approximations," *IEEE Transactions on Automatic Control*, vol. 48, pp. 246–258, Feb 2003.

[11] Y. Kim, N. A. Samad, K. Y. Oh, J. B. Siegel, B. I. Epureanu, and A. G. Stefanopoulou, "Estimating state-of-charge imbalance of batteries using force measurements," in *2016 American Control Conference (ACC)*, pp. 1500–1505, July 2016.

[12] M. Safari and C. Delacourt, "Modeling of a commercial graphite/lifepo4 cell," *Journal of The Electrochemical Society*, vol. 158, no. 5, pp. A562–A571, 2011.

[13] S. Mohan, Y. Kim, and A. G. Stefanopoulou, "Estimating the power capability of li-ion batteries using informationally partitioned estimators," *IEEE Transactions on Control Systems Technology*, vol. 24, pp. 1643–1654, sep 2016.